PCCP

Cite this: *Phys. Chem. Chem. Phys.*, 2012, **14**, 4355–4358

www.rsc.org/pccp

COMMUNICATION

Spectroscopic selection of distance measurements in a protein dimer with mixed nitroxide and Gd^{3+} spin labels†

Ilia Kaminker,[a] Hiromasa Yagi,[b] Thomas Huber,[b] Akiva Feintuch,[a] Gottfried Otting*[b] and Daniella Goldfarb*[a]

Received 22nd January 2012, Accepted 13th February 2012
DOI: 10.1039/c2cp40219j

The pulse DEER (Double Electron–Electron Resonance) technique is frequently applied for measuring nanometer distances between specific sites in biological macromolecules. In this work we extend the applicability of this method to high field distance measurements in a protein assembly with mixed spin labels, *i.e.* a nitroxide spin label and a Gd^{3+} tag. We demonstrate the possibility of spectroscopic selection of distance distributions between two nitroxide spin labels, a nitroxide spin label and a Gd^{3+} ion, and two Gd^{3+} ions. Gd^{3+}–nitroxide DEER measurements possess high potential for W-band long range distance measurements (6 nm) by combining high sensitivity with ease of data analysis, subject to some instrumental improvements.

The pulse DEER (Double Electron–Electron Resonance) experiment,[1–3] also known as PELDOR (Pulsed Electron Double Resonance), has become very popular in recent years for measuring nanometer distances in biological macromolecules in structural biology applications.[4–7] The most common application of DEER is to measure distances between two nitroxide spin labels (SLs) attached at specific points in the macromolecule of interest. Effective methods to attach nitroxide SLs to both proteins[8] and nucleic acids[9–12] have been developed and applied extensively.

High field, W-band (95 GHz, ~3.5 T) DEER measurements are advantageous compared to conventional measurements at X-band (9.5 GHz) frequencies mainly due to increased sensitivity, provided that the necessary microwave (MW) power is available.[13,14] W-band measurements require an order of magnitude smaller sample sizes than measurements at X-band at comparable concentrations,[13] or two orders of magnitude lower concentrations with a ~3–5 fold increased sample size, depending on the experimental set-up.[14] At W-band frequencies, however, the *g*-anisotropy of nitroxide SLs is resolved, which, together with the limited bandwidth of the microwave pulses, lead to orientation selection effects in the DEER traces.[15] Such orientation selective measurements allow the determination of the relative orientations of the *g*-tensors of the paramagnetic centers, in addition to the distance between them.[15–17] In many instances, however, the relative orientation of the SLs is not of great importance because they are attached to the biomolecule through a flexible linker and orientation selection only complicates the extraction of reliable distance distributions. To circumvent this difficulty, without having to compromise on the high sensitivity offered by high fields, a new class of SLs based on Gd^{3+} chelates has recently been proposed and implemented.[13,18,19]

The high-spin Gd^{3+} ($S = 7/2$) SLs were shown to behave similarly to $S = 1/2$ SLs in DEER measurements,[18] allowing the use of well-established data analysis procedures developed for the $S = 1/2$ case. Distance measurements utilizing Gd^{3+} based SLs reaching up to ~6 nm were recently reported for both a DNA duplex[19] and a protein homodimer.[20]

The best performing Gd^{3+} chelates used so far are rather large and therefore limited to labeling surface sites on proteins. Consequently, it is of interest to consider a situation where a buried site in the protein is labeled with a small nitroxide and the surface site with a bulky Gd^{3+} tag. Furthermore, to solve complex biochemical problems involving an assembly of proteins, it is sometimes beneficial to use more than a single type of spin label. Such complex labeling schemes enable the measurement of more than a single distance on the same sample with additional resolution based on spectroscopic selection of different pairs of labels. This approach was previously demonstrated on a mixture of ^{15}N and ^{14}N nitroxide based biradicals[21] and between copper(II) and a nitroxide on a model compound.[22] Such an approach also distinguishes between homo- and hetero-dimers.

The potential of DEER distance measurements between a nitroxide SL and a Gd^{3+} ion was recently demonstrated on a model compound with a rigid spacer and a Gd^{3+}–nitroxide distance of ~2.5 nm, using X-band and Q-band (34 GHz) spectrometers.[23] At W-band such an orthogonal spin labeled system should exhibit orientation selection only due to the nitroxide because of the isotropic *g* of Gd^{3+}, the isotropic character of its central transition (to second order), and the large distribution of its zero field splitting (ZFS).[24] Because of this broad distribution setting the pump or observer pulse to the broad, featureless background of the Gd^{3+} spectrum that includes contributions from all Gd^{3+} transitions, except the

[a] *Department of Chemical Physics, Weizmann Institute of Science, Rehovot 76100, Israel. E-mail: Daniella.goldfarb@weizmann.ac.il, go@rsc.anu.edu.au*
[b] *Research School of Chemistry, Australian National University, Canberra, ACT 0200, Australia*

† Electronic supplementary information (ESI) available: X-band CW EPR data, details of the DEER data analysis, quantitative description of the echo reduction effect. See DOI: 10.1039/c2cp40219j

central transition, with relative intensities determined by the Boltzmann distribution, there is no orientation selection for virtually any position in the Gd^{3+} spectrum.[18–20,24] Accordingly, the DEER data analysis needs to include only two angles, which define the orientation of the inter-spin vector with respect to the *g*-principal axis system of the nitroxide. This is a significant simplification compared to the case of two nitroxides where five angles need to be considered.[15] In proteins, the existence of orientation selection depends on the extent of mobility of the SL, which is a function of the protein local motion and the flexibility of the SL tether. This mobility translates into an orientation and distance distribution upon freezing. For highly flexible SLs positioned on surface sites of the protein there is no orientation selection, as all orientations are sampled and the data can be treated with the same procedures that are commonly applied for the treatment of X-band nitroxide DEER data.[5,6,13]

In this work we demonstrate the applicability of high field (W-band) DEER distance measurements to a protein assembly, the 51 kDa homodimer of the ERp29 chaperone, with nitroxide–Gd^{3+} labeling. For the present set of experiments we used the ERp29 S114C/C157S double mutant with a C1-Gd^{3+} tag described previously.[20,25] The preparation of the sample with a nitroxide label is described in the ESI.† The reagents used to spin label the protein are shown in Fig. 1. The final sample consisted of a mixture of 0.1 mM spin labeled ERp29 dimers with the following SL composition: two Gd^{3+} tags (25%), two nitroxide labels (25%), and one nitroxide and one Gd^{3+} tag (50%). By choosing the appropriate experimental conditions we selected Gd^{3+}–nitroxide, nitroxide–nitroxide, and Gd^{3+}–Gd^{3+} distances.

Optimizing experimental conditions for W-band Gd^{3+}–nitroxide DEER measurements. When performing pulse EPR measurements

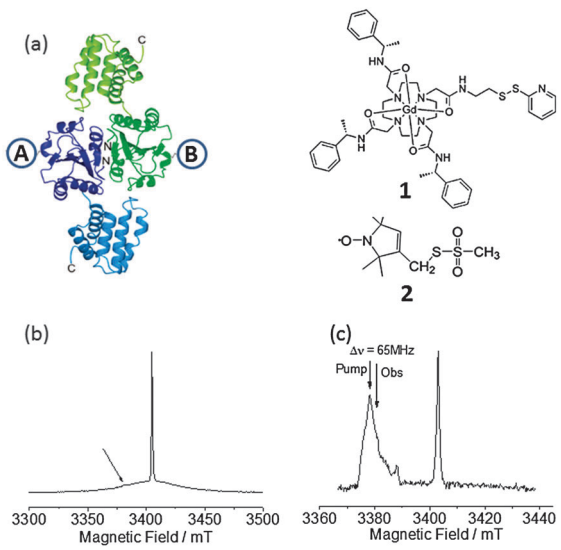

Fig. 1 (a) Structure of the ERp29 dimer (PDB ID 2QC7) showing the labeling sites and the spin labels C1-Gd^{3+}[25] (**1**) and MTSL (**2**) used in this study. Sample composition: 25% $A = B =$ **1**; 50% $A =$ **1**; $B =$ **2**; 25% $A = B =$ **2**. (b) and (c) ED-EPR spectra of the ERp29 dimer acquired with MW power optimized for Gd^{3+} (b) and for the nitroxide SL (c). Other experimental parameters were the same for both spectra: $\pi/2$ and π pulse durations were 60 ns and 120 ns, respectively; $\tau = 550$ ns; $T = 10$ K; repetition time: 50 ms.

on a pair comprising a nitroxide with $S = 1/2$ and a Gd^{3+} with $S = 7/2$, their considerably different spin physics characteristics have to be considered. The spin-lattice relaxation time of Gd^{3+} is several orders of magnitude shorter than that of the nitroxide ($\sim$100 μs and $\sim$100 ms, respectively, at 10 K) and the transition probabilities of Gd^{3+} are larger. Accordingly, at a given MW power, the π and $\pi/2$ MW pulses are much shorter for Gd^{3+} than for nitroxides. This allows selective distance measurements.

Fig. 1b shows the 10 K ED (Echo Detected) EPR spectrum of the mixed labeled ERp29 sample recorded under conditions optimized for Gd^{3+}. The spectrum consists of a sharp, $\sim$1.1 mT wide line due to the central $|-1/2\rangle \rightarrow |1/2\rangle$ transition, superimposed on a broad background arising from all other transitions. The contribution from the nitroxide spectrum (marked by an arrow in Fig. 1b) is barely observable under these conditions due to insufficient MW power. Fig. 1c shows the spectrum of the same sample acquired under MW power optimized for the nitroxide. Under these conditions, the signal of the nitroxide spectrum is strong and the Gd^{3+} signal is attenuated.

The pairwise time evolution of the echo intensity in a DEER experiment is given by:[1–3]

$$V(t) = V_0(1 - \lambda(1 - \cos\omega_d(1 - 3\cos^2\theta)t)); \qquad \omega_d = \frac{g_1 g_2 \beta^2 \mu_0}{4\pi h r^3} \tag{1}$$

where V_0 is the echo intensity at $t = 0$, g_1, g_2 are the g values, r is the inter-electron distance, and θ is the angle between the inter-electron vector and the magnetic field.

The modulation depth, λ, for a pumped nitroxide is given by:

$$\lambda = \int_{-\infty}^{\infty} \frac{\omega_1^2}{\omega_1^2 + \Delta\omega^2} \sin^2\left(\frac{t_p\sqrt{(\omega_1^2 + \Delta\omega^2)}}{2}\right) g(\Delta\omega) d(\Delta\omega) \tag{2}$$

where ω_1 and t_p are the amplitude and duration of the pump pulse, respectively, $\Delta\omega$ is the off-resonance frequency, and $g(\Delta\omega)$ is the lineshape of the nitroxide EPR spectrum. Eqn (1) and (2) are valid when there is no orientation selection, namely λ is orientation independent. For Gd^{3+}, λ has to be scaled by the relative populations of the $M_S = \pm 1/2$ levels in the case that the pump pulse is set to the central transition of the Gd^{3+} spectrum and $g(\Delta,\omega)$ corresponds to the lineshape of the central transition.[18] The signal to noise ratio (S/N) relevant for DEER is given by:[6]

$$S/N \propto V_0 \lambda \exp\left(\frac{-t_{exp}}{T_{m(obs)}}\right) \frac{1}{\sqrt{T_{1(obs)}}} \tag{3}$$

where $T_{m(obs)}$ and $T_{1(obs)}$ are the phase memory time and the spin-lattice relaxation time of the observer spins, and t_{exp} is the time between the first pulse and the refocused echo in the four pulse DEER experiment[1] (see Fig. S2, ESI†). According to eqn (3), the nitroxide–Gd^{3+} distance is measured best by setting the observer frequency to the central transition of the Gd^{3+} spectrum to obtain a large V_0 that can be accumulated very fast due to the short T_1. The pump pulse should be set to the nitroxide spectrum to achieve a large λ because the nitroxide spectrum is narrower.[23] We note that the T_1 of the pumped spins is irrelevant as long as it is not too short.

The separation between the maximum of the $|-1/2\rangle \rightarrow |1/2\rangle$ transition of the Gd^{3+} spectrum and the maximum of the

nitroxide spectrum at W-band is $\Delta\nu$ = 685 MHz (Fig. 1c). Unfortunately, this is larger than the bandwidth of our current cavity ($\sim$100 MHz). We therefore chose a configuration with $\Delta\nu$ < 100 MHz, setting the observer pulse to the broad background of the Gd^{3+} spectrum as shown in Fig. 1c, thus considerably compromising V_0 (by a factor of about 20) and reducing the signal-to-noise (S/N) ratio according to eqn (3). In this configuration, pulses given at the observer frequency affect, in principle, both the Gd^{3+} and nitroxide spins. The latter, however, were suppressed by using a high repetition rate (5 kHz) that saturates the observer nitroxide spins due to their much longer T_1 at 10 K.

Our chosen experimental configuration with $\Delta\nu$ = 65 MHz created a very strong direct off-resonance effect of the pump pulse on the observer spins, resulting in a significant reduction of V_0. This effect is similar to the phase shift effect described earlier[27] but is much more pronounced due to the high transition probability of the high-spin Gd^{3+} ion. A pump pulse with a flip angle of π for the nitroxide spins amounts to a $\sim 4\pi$ pulse for the Gd^{3+} spins. This difference produced a much stronger echo reduction compared to the situation of DEER applied to two nitroxide or two Gd^{3+} labels, where the echo reduction effect is practically negligible. This effect is described and analyzed in detail in the ESI.† To obtain DEER data with an acceptable S/N ratio, we reduced the duration of the pump pulse until V_0 was within $\sim$70% of its initial intensity without the pump pulse.

DEER distance measurements. The Gd^{3+}–nitroxide four-pulse DEER data after the background subtraction are shown in Fig. 2a. The experiment was performed with a pump frequency, ν_{pump}, set to the maximum of the nitroxide spectrum and the observer frequency set to $\nu_{obs} = \nu_{pump} + 65$ MHz. At this spectral position, many orientations are excited simultaneously. Moreover, the X-band room temperature EPR spectrum (Fig. S1, ESI†) indicates a relatively unconstrained motion of the nitroxide spin SL at room temperature. This suggests little orientation selection at low temperatures. Accordingly, we proceeded to analyse the data neglecting orientation selection, using the common approach used for X-band DEER data (eqn (1) and (2)). The resulting distance distribution is shown in Fig. 2a. Details of the background subtraction procedure and data analysis are available in the ESI.† The distance distribution shows a maximum at 5.86 nm.

Next we measured the distances in the ERp29 dimers labeled with two C1-Gd^{3+} SLs (25%). To exclude the nitroxide spins from the DEER experiment, we set both the observer and the pump frequencies outside of the nitroxide EPR spectrum. The observer frequency was set to the maximum of the $|-1/2\rangle \rightarrow |1/2\rangle$ Gd^{3+} transition to maximize V_0 and the pump frequency was set to $\nu_{pump} = \nu_{obs} + 65$ MHz. The distance distribution shown in Fig. 2b (right) has a maximum at 6.04 nm. This is identical to the distance measured in the previous work on the pure C1-Gd^{3+} labeled sample.[20]

Finally we measured the nitroxide–nitroxide distance in the ERp29 dimers with two nitroxide spin labels (25%). There is no range in the nitroxide EPR spectrum without overlap with the Gd^{3+} signal. Therefore we took advantage of the different relaxation properties of the two paramagnetic centers and carried out the measurements at 50 K, where the Gd^{3+} contribution to the EPR spectrum becomes negligible. The measurements were

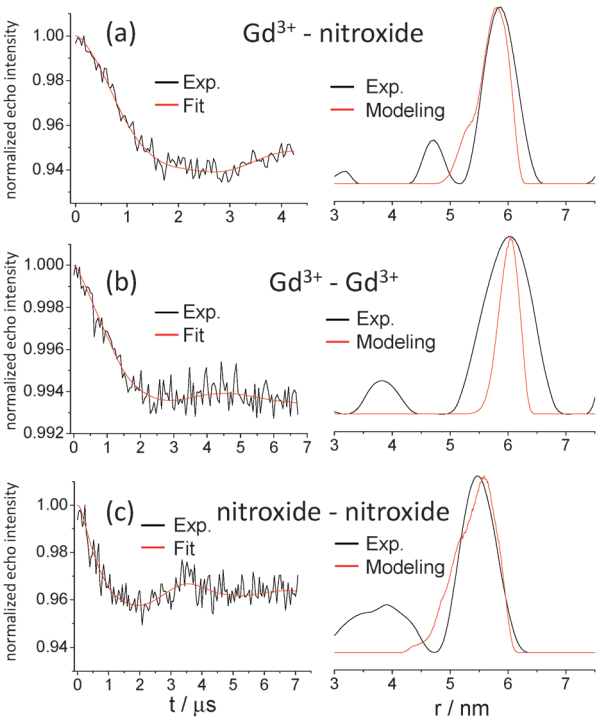

Fig. 2 DEER results of mixed labeled ERP29 dimers at 10 K. Left panel: DEER traces after background removal with fits obtained with the distance distributions shown on the right. Right panel: distance distributions obtained by Tikhonov regularization (regularization parameter: (a) α = 100; (b, c) α = 1000) using the DEER Analysis software[26] and modeling. (a) Gd^{3+}–nitroxide experiment. Experimental parameters: repetition rate 5 kHz, pump pulse duration t_p = 17.5 ns ($\sim$130° pulse for the nitroxide spins), observer pulse durations $t_{o,\pi/2}$ = 30 ns and $t_{o,\pi}$ = 60 ns; (b) Gd^{3+}–Gd^{3+} experiment. Repetition rate 5 kHz, t_p = 15 ns, $t_{o,\pi/2}$ = 30 ns, $t_{o,\pi}$ = 60 ns. (c) Nitroxide–nitroxide distance measurement. A sum of two DEER traces measured with $\Delta\nu = \pm 65$ MHz, t_p = 30 ns, $t_{o,\pi/2}$ = 50–55 ns, $t_{o,\pi}$ = 100–110 ns. Repetition rate 0.2 kHz, Accumulation times of the DEER traces in (a, b) were 7 h and 8 h, respectively. Individual traces in (c) were accumulated for 26 hours and 15 hours for $\Delta\nu = +65$ MHz and $\Delta\nu = -65$ MHz respectively. More experimental details for the trace and data analysis procedures are given in the ESI.†

carried out at two observer frequencies and the two separate traces are shown in Fig. S4 (ESI†). Assuming that the two acquired DEER measurements sample most of the available distances (see the ESI† for details) we summed the two DEER datasets. Fig. 2c (left) shows the combined DEER trace after the background subtraction. This gave a nitroxide–nitroxide distance distribution with a maximum at 5.5 nm (Fig. 2c, right). The modulation depth in all three types of distance measurements is lower than expected from eqn (2) because of the statistical nature of the spin labeling.

We carried out model calculations based on the crystal structure of ERp29 (PDB ID 2QC7) to account for the experimentally determined Gd^{3+}–nitroxide and the nitroxide–nitroxide distance distributions. Our recent Gd^{3+}–Gd^{3+} distance measurements showed that this structure prevails also in solution.[20] The distance distributions were modeled by crafting the spin labels onto the cysteine residues, randomly varying the dihedral angles, and eliminating those rotamers that had steric clashes with the protein. A comparison of the experimental and

calculated distance distributions of the different pairs of spin labels is shown on the right side of Fig. 2. The substitution of one of the C1-Gd^{3+} tags by a nitroxide spin label shifts the maximum of the calculated distance distribution from 6.05 nm[20] to 5.81 nm. Substitution of the second Gd^{3+} tag by the nitroxide SL shortens the distance further to 5.6 nm. These shifts in the maxima of the calculated distance distributions agree well with the experimental results. The largest discrepancy (no more than 0.1 nm) is observed for the nitroxide–nitroxide distance distribution.

The modelled distance distribution is the narrowest for two C1-Gd^{3+} tags, whereas it becomes broader when one C1 tag is changed to a nitroxide SL and broadens even further upon the second substitution. This reflects the larger conformational space sampled by the nitroxide SL compared to the bulky C1-Gd^{3+} tag, which positions the Gd^{3+} ion in a more well defined location relative to the protein. This trend is not reproduced experimentally, which may be attributed to S/N limitations and the insufficiently long evolution time in the nitroxide–Gd^{3+} DEER measurements. Alternatively, the conformational sampling of the nitroxide SL may be non-uniform due to its hydrophobicity.

The present work shows that we can spectroscopically select Gd^{3+}–Gd^{3+}, nitroxide–Gd^{3+}, and nitroxide–nitroxide distance distributions, in the range of 6 nm, from a mixed labeled protein dimer using a very small quantity of protein (about 0.3 nmol in total). We note that the effective concentration of the homo-labeled dimers was only 25 μM and the sample size is 2–3 μL. As shown from eqn (3), the S/N ratio in the DEER experiment depends on both the modulation depth λ and the echo intensity formed by the observer spins, V_0. This allows the orthogonal Gd^{3+}–nitroxide DEER experiment to combine the larger modulation depth of the nitroxide–nitroxide measurement with the high signal intensity and fast repetition rate of the Gd^{3+}–Gd^{3+} measurements. In principle, the echo intensity, V_0, in the Gd^{3+}–nitroxide experiment is larger than that of the corresponding Gd^{3+}–Gd^{3+} measurement, since one can benefit from the full intensity of the $|-1/2\rangle \rightarrow |1/2\rangle$ transition that is usually utilized as pump spins in the conventional Gd^{3+}–Gd^{3+} DEER measurement. Performing this experiment in the optimal way requires about 700 MHz separation between the observer and pump frequencies. Such a large frequency separation will also eliminate the direct off-resonance effects of the pump pulse on the observed echo described earlier. Such a large frequency separation is usually not feasible for the narrow band cavities used in most W-band EPR spectrometers. This limitation can be overcome either by using an extremely high-power MW source which allows for sufficiently strong MW pulses even in the absence of a cavity[14] or by utilizing a dual mode resonator as reported recently.[28] We expect that the Gd–nitroxide DEER sensitivity will increase by a factor of 20–40 with such a cavity.

When there is no interest to measure several distances from a single sample, realization of the full S/N advantage of the Gd^{3+}–nitroxide DEER measurement requires preparation of a sample in which 100% of the molecules of interest are labeled with both types of paramagnetic centers. This is readily achieved with heterodimers, where each monomer can be labeled separately with a different type of spin label. If an intramolecular distance is of interest, it is possible to utilize labeling schemes where two different labels are attached to the same molecule as is common for FRET (Förster Resonance Energy Transfer) experiments. Random labeling will lead to Gd^{3+}–nitroxide pairs in only 50% of the sample as in the case of ERp29 shown here.

Acknowledgements

G. O. and T. H. acknowledge grant support and a Future Fellowship for T. H. from the Australian Research Council. This research was supported by the Israel Science Foundation (ISF) and was made possible in part by the historic generosity of the Harold Perlman family (D. G.). D. G. holds the Erich Klieger Professorial Chair in Chemical Physics.

Notes and references

1 M. Pannier, S. Veit, A. Godt, G. Jeschke and H. W. Spiess, *J. Magn. Reson.*, 2000, **142**, 331–340.
2 A. D. Milov, A. B. Ponomarev and Y. D. Tsvetkov, *Chem. Phys. Lett.*, 1984, **110**, 67–72.
3 R. G. Larsen and D. J. Singel, *J. Chem. Phys.*, 1993, **98**, 5134–5146.
4 C. S. Klug and J. B. Feix, *Biophysical Tools for Biologists, Volume One: In vitro Techniques*, Academic Press, 2008, vol. 84, pp. 617–658.
5 P. P. Borbat and J. H. Freed, *Two-Component Signaling Systems, Part B, Meth. Enzymol.*, Academic Press, 2007, vol. 423, pp. 52–116.
6 G. Jeschke and Y. Polyhach, *Phys. Chem. Chem. Phys.*, 2007, **9**, 1895–1910.
7 O. Schiemann and T. F. Prisner, *Q. Rev. Biophys.*, 2007, **40**, 1–53.
8 W. L. Hubbell, A. Gross, R. Langen and M. A. Lietzow, *Curr. Opin. Struct. Biol.*, 1998, **8**, 649–656.
9 P. Z. Qin, I. S. Haworth, Q. Cai, A. K. Kusnetzow, G. P. G. Grant, E. A. Price, G. Z. Sowa, A. Popova, B. Herreros and H. He, *Nat. Protocols*, 2007, **2**, 2354–2365.
10 T. E. Edwards and S. T. Sigurdsson, *Nat. Protocols*, 2007, **2**, 1954–1962.
11 O. Schiemann, N. Piton, J. Plackmeyer, B. E. Bode, T. F. Prisner and J. W. Engels, *Nat. Protocols*, 2007, **2**, 904–923.
12 X. Zhang, P. Cekan, S. T. Sigurdsson and P. Z. Qin, *Biophysical, Chemical, and Functional Probes of RNA Structure, Interactions and Folding: Part B, Meth. Enzymol.*, Academic Press, 2009, vol. 469, pp. 303–328.
13 A. Potapov, H. Yagi, T. Huber, S. Jergic, N. E. Dixon, G. Otting and D. Goldfarb, *J. Am. Chem. Soc.*, 2010, **132**, 9040–9048.
14 P. A. S. Cruickshank, D. R. Bolton, D. A. Robertson, R. I. Hunter, R. J. Wylde and G. M. Smith, *Rev. Sci. Instrum.*, 2009, **80**, 103102.
15 Y. Polyhach, A. Godt, C. Bauer and G. Jeschke, *J. Magn. Reson.*, 2007, **185**, 118–129.
16 V. P. Denysenkov, T. F. Prisner, J. Stubbe and M. Bennati, *Proc. Natl. Acad. Sci. U. S. A.*, 2006, **103**, 13386–13390.
17 Z. Yang, D. Kise and S. Saxena, *J. Phys. Chem. B*, 2010, **114**, 6165–6174.
18 A. M. Raitsimring, C. Gunanathan, A. Potapov, I. Efremenko, J. M. L. Martin, D. Milstein and D. Goldfarb, *J. Am. Chem. Soc.*, 2007, **129**, 14138–14139.
19 Y. Song, T. J. Meade, A. V. Astashkin, E. L. Klein, J. H. Enemark and A. Raitsimring, *J. Magn. Reson.*, 2011, **210**, 59–68.
20 H. Yagi, D. Banerjee, B. Graham, T. Huber, D. Goldfarb and G. Otting, *J. Am. Chem. Soc.*, 2011, **133**, 10418–10421.
21 G. Jeschke, H. Zimmermann and A. Godt, *J. Magn. Reson.*, 2006, **180**, 137–146.
22 E. Narr, A. Godt and G. Jeschke, *Angew. Chem., Int. Ed.*, 2002, **41**, 3907–3910.
23 P. Lueders, G. Jeschke and M. Yulikov, *Phys. Chem. Lett.*, 2011, **2**, 604–609.
24 A. Raitsimring, A. Astashkin, O. Poluektov and P. Caravan, *Appl. Magn. Reson.*, 2005, **28**, 281–295.
25 B. Graham, C. T. Loh, J. D. Swarbrick, P. Ung, J. Shin, H. Yagi, X. Jia, S. Chhabra, N. Barlow, G. Pintacuda, T. Huber and G. Otting, *Bioconj. Chem.*, 2011, **22**, 2118–2125.
26 G. Jeschke, V. Chechik, P. Ionita, A. Godt, H. Zimmermann, J. Banham, C. R. Timmel, D. Hilger and H. Jung, *Appl. Magn. Reson.*, 2006, **30**, 473–498.
27 M. K. Bowman and A. G. Maryasov, *J. Magn. Reson.*, 2007, **185**, 270–282.
28 I. Tkach, G. Sicoli, C. Höbartner and M. Bennati, *J. Magn. Reson.*, 2011, **209**, 341–346.

